Experimental Study of Dual Bell Nozzles

C. Nürnberger-Génin and R. Stark
DLR, German Aerospace Center, Lampoldshausen,
D-74239, Germany

Abstract
An experimental study was conducted testing Dual-bell nozzles in various conditions at DLR's cold gas test stand. The stability of the nozzle flow has been verified by measuring the pressure ratio values by flow transition and retransition, to ensure a hysteresis between the two operation modes. The transition duration and the velocity of the transition front in the nozzle extension were calculated using pressure measurement and Schlieren optics to demonstrate the feasibility of the Dual-Bell concept.

1. Introduction

For Europe's heavy launcher Ariane 5 the stage design was changed from classical tandem to a parallel configuration and its main stage engine Vulcain 2 therefore has to fulfil a wider range of operation conditions during ascent. For this reason the rocket engine's nozzle comes into focus as the sub system with the most promising performance gain. Vulcain's current nozzle is designed to be full flowing under sea-level conditions to avoid flow separation and resulting undesired side loads. But this limits the expansion area ratio and results in performance losses as ambient pressure decreases during ascent meaning large parts of the trajectory feature vacuum conditions.
The European Flow Separation Control Device group (FSCD) was initiated to study both flow separation in classical bell nozzles and altitude adapting rocket nozzles such as plug nozzles, dual-bell nozzles or nozzles with an extendible exit cone. As a result the dual bell nozzle was identified as the most promising concept.

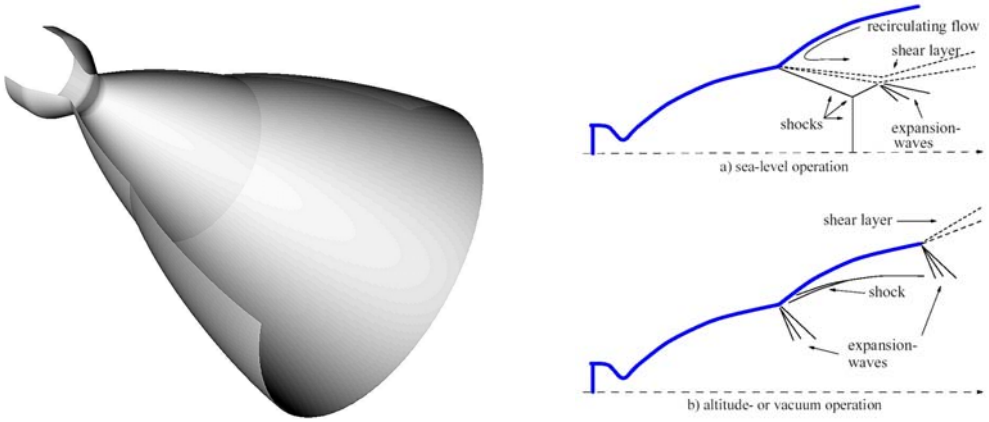

Figure 1 : (a) Dual-Bell nozzle and (b) Nozzle flow at sea level (top) and high altitude operation (bottom)

The dual-bell nozzle operates under sea-level and high altitude conditions. Its characteristic wall inflection, dividing the nozzle into base and extension, offers a one-step altitude adaptation, without any moving parts. In sea-level mode, the wall inflection forces the flow to separates controlled and symmetrically, dangerous side loads are avoided and due to a smaller effective area ratio the sea-level thrust increases. During ascent of the launcher, at a certain altitude, the nozzle flow attaches to the wall of the nozzle extension until the exit plane. The full (higher) expansion area ratio is used resulting in a higher vacuum performance.
With its classical and easy bell design of base nozzle and nozzle extension only a few changes on existing rocket engines become necessary. Compared to other advanced nozzle concepts, the absence of any mechanical part which would increases its weight is one of the outstanding features.

The concept was first mentioned in 1949 by Foster and Cowles[1] as an alternative to conventional nozzles in a flow separation study. The first tests were conducted at Rocketdyne Division by Horn and Fisher[2] in 1994. Since the early

nineties, many studies, mostly numerical, have been made by Goel and Jensen[3], Hagemann et.al.[4], Immich and Caporicci[5] (within the FESTIP program) to understand and attempted to predict the behavior of this new nozzle concept. A numerical study of the feasibility was made by Karl and Hanemann[11]. Calculations were made to verify the transition duration and stability of the flow in Dual-Bell nozzles.

2. Presentation of the test facility and test objectives

2.3 Test facility

The test facility P6.2 at the DLR Lampoldshausen features cold flow testing of sub-scale nozzles and ejectors. The test bench consists of two areas: the altitude simulation chamber with a self-evacuating system to study the nozzles behavior at low ambient pressure, and a horizontal rig for the testing at sea-level conditions (see also ref. [6] and [11]). This Dual-Bell nozzle study was performed on the horizontal rig (see fig. 2), with variable feeding pressure.

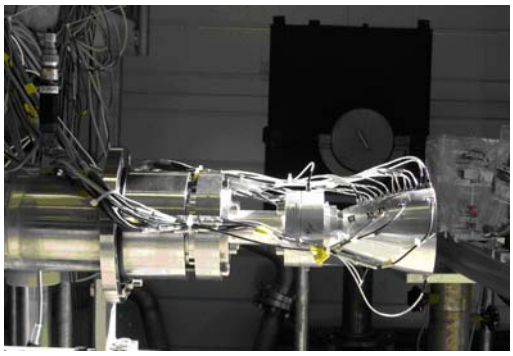

Figure 2 : Dual-Bell model on the horizontal rig

Nitrogen was used as feeding gas for the test series. The ambient pressure P_a was constant for the whole test series at 1bar. The nozzle pressure ratio (NPR) P_0/P_a was adjusted by varying the feeding pressure P_0 of the nozzle.

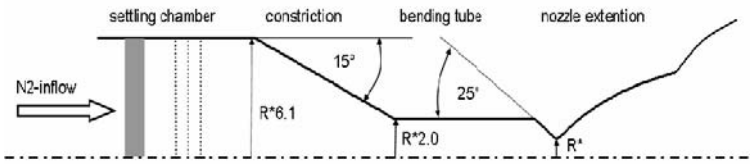

Figure 3 : Test rig geometry

The base contour of the tested nozzle was designed as a truncated ideal contour (TIC). The extension was designed on the isobar leaving the last point of the base nozzle using the method of the characteristics featuring a constant pressure (CP) wall profile. The geometric parameters are summarized in the table 1 and the geometry of the subsonic part is represented in the figure 3.

Table 1 : Nozzle geometry

Throat radius	$R^* = 0.01$m
Area ratio	$\varepsilon_1 = 11.3$ $\varepsilon_2 = 27,1$
Nozzle length	Lbase/Rth = 6.2 Lext/Rth = 8.3
Contour angle	$\alpha = 9°$

2.2 Measurements

For each test, the wall pressure P_w along the nozzle, and the total pressure respectively the total temperature T_0 were measured. The wall pressure variations are measured using both high (HF) and low (LF) frequency XT-154-190M Kulite pressure sensors, with a scan rate of 25 kHz and 1000 Hz respectively and related analogue cut-off

frequencies of 8 kHz and 160 Hz. The positions of the measurements points are illustrated on figure 4 left. The HF pressure sensors are located along the extension wall, to detect the transition front by the change of mode. The repartition of the HF and LF sensors on the nozzle wall is shown in figure 4 b). A schlieren optics installation with a high speed camera took images of the nozzle exhaust flow with a frequency of 2kHz.

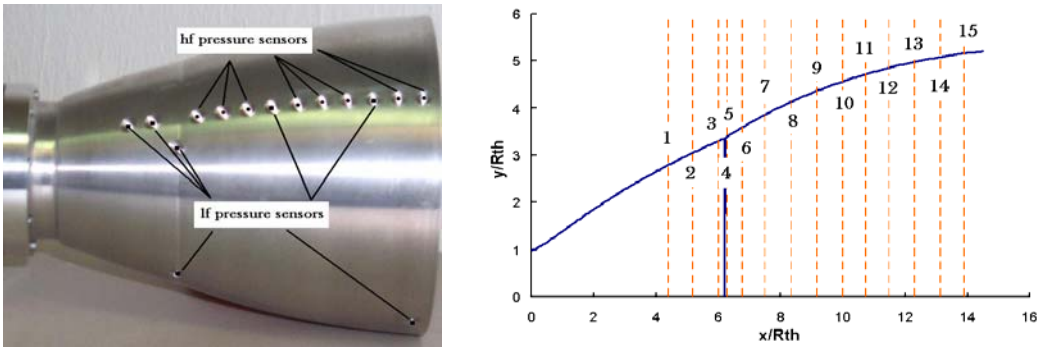

Figure 4 : a) Dual-Bell on the testing bench and b) pressure sensor positions

2.3 Test logic

The figure 3 is an example of the pressure profile of a test session. The feeding pressure P_0 was increased and decreased with a constant gradient to study its effect on the transition conditions. The evolution of the wall pressure in the extension is also represented in figure 5 (P_{wext}). At low values of P_0, the flow separates at the inflection and the pressure measured in the extension corresponds to the flow recirculation pressure, which is between 92 and 98% of the ambient pressure. This value represents the pressure measured in separation zone by conventional nozzles (see ref. [9] and [10]). If the pressure increases, the wall pressure drops suddenly as the flow attaches to the extension wall. By decreasing the pressure again, the wall pressure in the extension jumps back to the recirculation pressure.

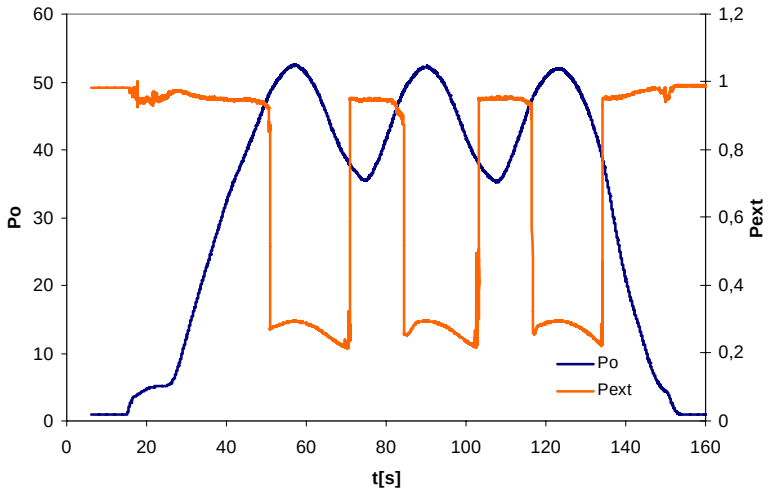

Figure 5 : Profile of feeding and wall pressure

The feeding pressure was recorded at the instant of the transition and the retransition to determine the hysteresis between the two operating modes of the dual bell nozzle.
The transition duration was determined using two methods. The first one is following the instant of the wall pressure drop along the nozzle extension. The duration is calculated between the first (downstream the inflection) and the last sensor (upstream the nozzle lip) within the extension. The second method uses the schlieren optics installation. The flow is recorded in intervals of 0.5ms. The pressure ratio is varied with different gradient to study its influence on the transition and retransition duration. Four test series have conducted with pressure gradients of 0.7bar/s, 1.2bar/s, 1.7bar/s and 2.2bar/s.

It has been seen by back dated cold gas tests and by numerical simulation made by Nasuti et.al.[10], that the velocity of the transition front is not constant. It starts slowly in the vicinity of the inflection, accelerates in the middle part and slows down again at the end of the nozzle. Therefore is the duration not the only parameter of importance to define the transition behavior. In fact, the side loads generated by the flow separation are function of the length of the instability zone (Δx), the ambient and wall pressure (resp. Pa and Pw) as shown in the equation (1): (Cf. Hagemann et. al.[3]).

$$Fs = (pa - pw)\pi r(s)\frac{pw(\delta_{up} + \delta_{low})}{2(\partial p / \partial x)} \qquad \textbf{(1)}$$

The worst case side loads can be calculated with the whole extension length as Δx, and during the whole transition duration. But the transition must be divided in three parts: in the vicinity of the inflection and at the end of the nozzle, the short length Δx limits the intensity of the side loads and in the central part, with a large value of Δx the side loads increases, but the duration is very short. To study this phenomenon, the velocity of the transition front has been measurement along the nozzle extension, using HF sensors.

3. Results and discussion

The figure 6 illustrates the wall pressure measurements obtained for the pressure ratios Po/Pa: 30, 48 and 51 compared to theoretical values calculated with the method of the characteristics for attached flow. At low pressure ratio (Po/Pa = 30), the flow attaches in the base nozzle and separates at the inflection. In the inflection region, the pressure increases to adjust to the ambient pressure, and reaches the recirculation pressure in the extension. As the pressure ratio Po/Pa increases to 48, the pressure gradient within the separation region decreases. As the nominal transition pressure ratio is reached, the flow jumps to the end of the nozzle. At a pressure ratio of 51, the flow attaches to the extension wall. The wall pressure is constant in the extension part, as foreseen by the calculation. The last measured point shows the typical end effect of highly overexpanded rocket nozzles.

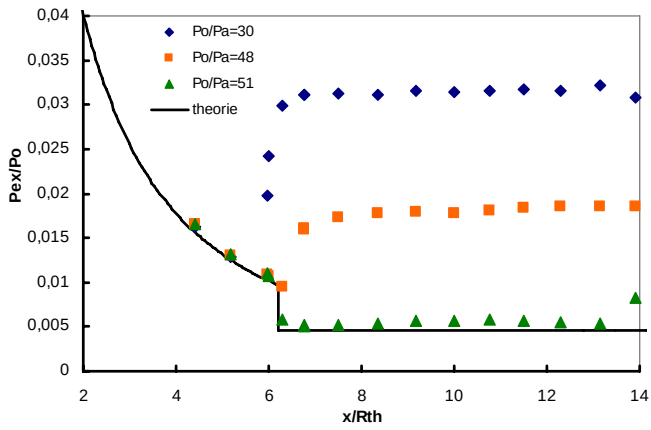

Figure 6 : Wall pressure distribution for various pressure ratios

3.1 Stability

To ensure a steady transition from one operating mode to the other, the nominal pressure ratio Po/Pa at the transition has to be clearly higher than the pressure ratio at the retransition. So that small variations of the pressure ratio due to ambient effects (buffeting) or combustion instabilities don't lead to an undesired retransition of the flow.

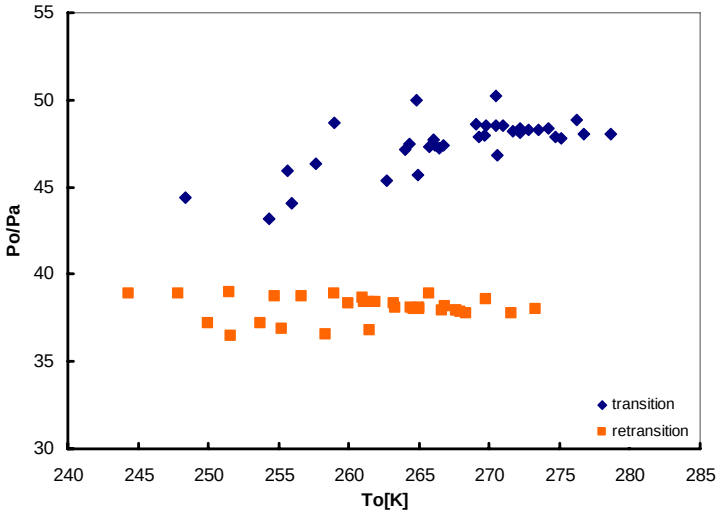

Figure 7 : Hysteresis effect between transition and retransition

The figure 7 presents the pressure ratio measured at the transition and at the retransition for each of the conducted test as a function of the total temperature. Both total temperature and pressure ratio are function of time; this representation gives the most clearly illustration of the hysteresis effect. An important difference can be seen between the nominal pressure ratio for transition and retransition. At low temperatures (To lower than 260K), the values of the NPR for the transition have to be taken with caution. These temperatures are due to a decreasing temperature in the outside the facility located storage vessels, when a quasi adiabatic expansion takes place. Indeed, at these temperatures, the condensed humidity of the air freezes at the wall surface (see picture on the figure 8). The ice thickness and its roughness influence the flow behavior: the transition occurs already for lower pressure ratio values.

Figure 8 : frozen surface of the nozzle model

The transition and retransition pressure ratio have been measured individually for each test of the campaign. The average NPR difference is around 20%. This will avoid instabilities between the operating modes in case of buffeting.

3.2 Transition duration

The duration of the transition and retransition has been measured using two methods. The wall pressure measurements give the evolution of the separation front moving in the extension by changing of mode. Schlieren optics yields a qualitative observation of the transition behavior.

3.2.1 Schlieren optics measurements

The exhaust flow of the nozzle was recorded using a Schlieren optics installation. The images are shot with an interval of 0.5ms. The figure 9 represents 6 consecutive images taken during the transition. On the first image (a), the flow still separates at the inflection. The visible exhaust plume is small (inflection area ratio) and the mach disc is

inside the nozzle extension. On the images (b), (c) and (d), the transition occurs: the mach disc moves downstream, outside of the nozzle. A slight asymmetry can be notice in the plume (tilted Mach disc), before the flow gets stabilized at the nozzle lip.

On the last image (f), the flow hasn't reached the end of the nozzle, and the mach disk is still close to the nozzle lip. This picture is yet taken as the last one of the transition, because the flow needs a lot of time to reach the nozzle lip, due to the contour imperfection.

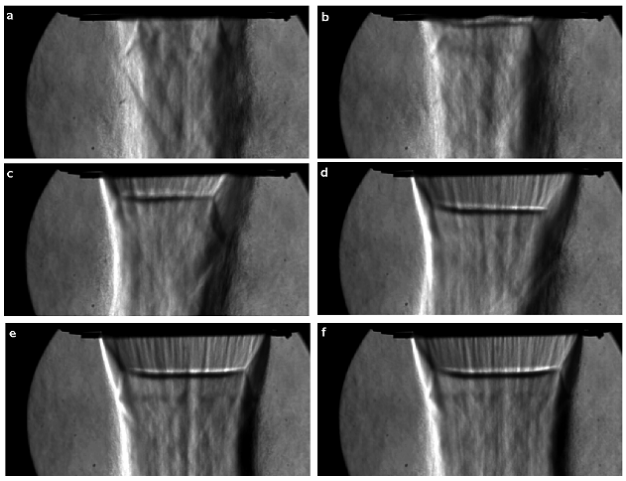

Figure 9 : Schlieren imaging of the flow transition

The duration of the transition (and retransition) is calculated between two stable positions of the jet: the last image on which the flow separates at the inflection up to the first image showing a stable attached flow. The duration is averaged for each series of similar tests (tab. 2).

3.2.2 Pressure measurements

The transition duration was determined using wall pressure measurements, too. The instant of the pressure drop in the extension is recorded for each sensor. Figure 6 illustrates the time history of transition (a) and retransition (b). The point of origin represents the contour inflection and corresponds actually to the second measurement point in the extension (sensor 6). The first sensor positioned in the extension is not taken in to account, because it is located direct at the inflection, and the transition front moves slowly in the inflection region before the beginning of the transition. Each point in the graph corresponds of the position of a HF measurement position along the nozzle extension and the instant at which it is reached by the separation front.

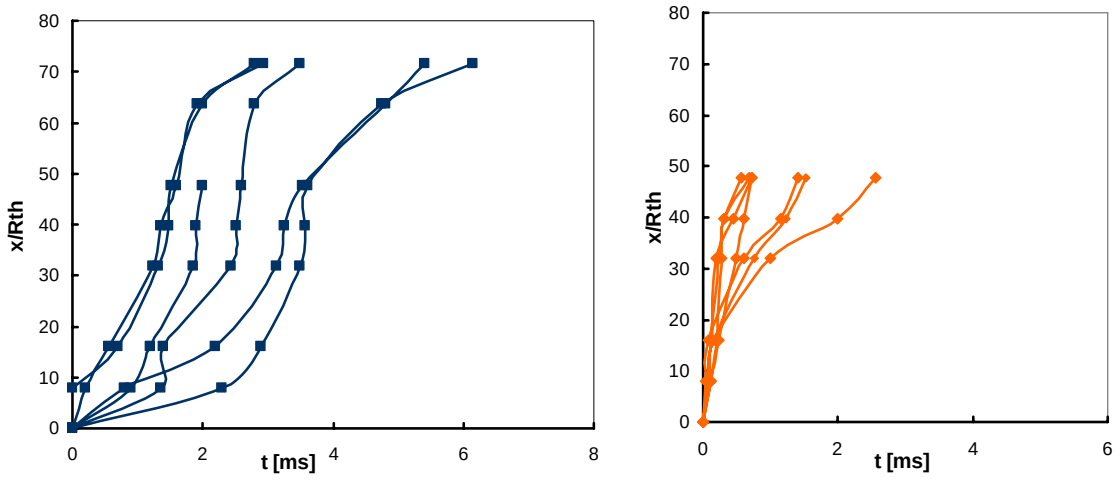

(a) (b)

Figure 10 : Transition (a) and retransition (b) duration

When the transition starts, the separation front lifts off slowly from the inflection and accelerates in the central part of the nozzle. The front slows down at the end of the extension again. This behaviour has been also seen by numerical studies[10].
By the retransition, the sensors positions 14 and 15 have been ignored because of the flow separation at the nozzle lip. The time history of the retransition is represented on the figure 10 (b).

Table 2 : Transition duration as a function of the pressure gradient

Pressure gradient	Transition duration	
$\Delta(P_0 / P_a) / \Delta t$	Pressure measurements	Schlieren optics
0,7 s^{-1}	4,85ms	4,83ms
1,2 s^{-1}	4,3ms	4,33ms
1,7 s^{-1}	4,22	

The values of the averaged transition duration obtained for both methods for various pressure gradients are summarized in the table 2. The transition and retransition duration decreases with increasing pressure ratio gradient. To ensure a fast transition on flight condition (e.g. Vulcain2), the combustion chamber pressure should be regulated, so that the pressure ratio changes abruptly. Lowing the combustion chamber pressure Po down to 60% will avoid a transition taking place in the buffeting region.

3.3 Front Velocity

As seen in the figure 10, the transition and retransition don't have the same time behavior. The transition must be divided into three parts: the flow moves slowly near the wall inflection, then accelerates in the extension and slows down again in the vicinity of the nozzle lip. In most of the extension, the transition front moves very fast. High frequency pressure measurement at the extension wall yield values for the front velocity calculation (between the positions 10 and 12, see figure 5). The retransition behavior can't be separated by the same way. As the pressure ratio decreases up to the retransition NPR, the flow moves to the contour inflection with increasing velocity. To calculate the velocity, the value has been measured between the same positions as by the transition. The velocity represents then the local front velocity and can be compared to the transition, but it is not the maximum front velocity.

Table 3 : Comparison of local front velocity with pressure gradient

Series	Pressure gradient	Transition [m/s]	Retransition [m/s]
1	0,7s^{-1}	39.9	8.6
2	1,2 s^{-1}	67.4	25.4
3	1,7 s^{-1}	83.1	29.8

The calculations are made for various values of the pressure gradient (i.e. the pressure ratio Po/Pa gradient). The values obtained for the pressure gradient of 0.7bar/s, 1.2bar/s and 1.7bar/s are summarized in the table below:

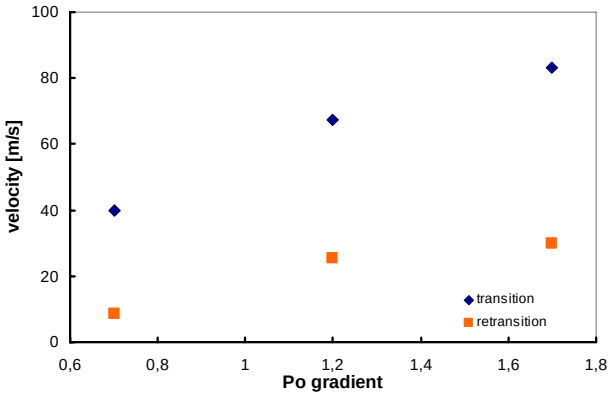

Figure 11 : Averaged front velocity for various pressure gradients

The local front velocity increases with the pressure gradient. The flow velocity at the nozzle wall attaints Mach 5.5 (690m/s). The figure 11 illustrates the transition and retransition front velocity as a function of the pressure gradient.

4. Summary

An experimental study has been made on the feasibility of the Dual-Bell nozzles. The cold tests on sub-scale nozzles have shown a good stability between the two operating modes through a hysteresis effect on the transition pressure ratio from up to 20%. The transition duration was measured with two methods: pressure measurements and Schlieren optics and is in order of a few milliseconds. Both methods have shown an influence of the pressure gradient on transition duration and local front velocity.

References

[1] Foster and Cowles, Experimental Study of Gas Flow Separation in Overexpanded Exhaust Nozzles for Rocket Motors, JPL Progress report 4-103, 1949.
[2] Horn, M. and Fisher, S., Dual-Bell Altitude Compensating Nozzles, Rocketdyne Division NASA-CR-194719, 1994.
[3] Goel, P. and Jensen, R., Numerical Analysis of the Performance of Altitude Compensating Dual-Bell Nozzle Flows, Rocketdyne Division, 1995.
[4] Hagemann, G., and Frey, M. and Manski, D., A critical Assessment of Dual-Bell Nozzles, AIAA 97-3299, 1997.
[5] Immich, H. and Caporicci, M.,FESTIP Technology Developments in Liquid Rocket Propulsion for Reusable Launch Vehicles, AIAA 96-3113, 1996.
[6] Stark, R., Boehm, C., Haidn, O. and Zimmermann, H., Cold Flow Testing of Dual-Bell Nozzles in Altitude Simulation Chambers, EUCASS, 2005.
[7] Alziary de Roquefort T., Low Frequency Fluctuations in Separated Turbulent Compressible Flows, Symposium on Advanced Fluid Information, Tohoku University, Japan, AFI 2002.
[8] Stark, R. and Wagner, B., Mach Disk Shape in Truncated Ideal Contour Nozzles, ISSW26 Symposium, 2007.
[9] Karl, S. and Hannemann, K., Numerical Investigation of Transient Flow Phenomena in Dual-Bell Nozzles.
[10] Nasuti, F., Onofri, F. and Martelli, E., Role of Wall Shape on the Transition in axisymmetric Dual-Bell Nozzles, AIAA-2003-4911, 2003.
[11] Kronmüller, H., Schäfer, K., Strak, R. and Zimmermann, H., Kaltgas-Höhensimulationsprüfstand P6.2 des DLR Lampoldshausen, DGLR, 2002.